Bcl-2 overexpression reduces cisplatin cytotoxicity by decreasing ER-mitochondrial Ca^{2+} signaling in SKOV3 cells

LU XU[1*], QI XIE[2*], LING QI[1], CHUNYAN WANG[1], NA XU[1], WEIMIN LIU[3], YANG YU[1], SONGYAN LI[1] and YE XU[1]

[1]Key Laboratory of Colleges and Universities of Jilin, College of Basic Medicine, Jilin Medical University, Jilin, Jilin 132013; [2]Department of Pathophysiology, College of Basic Medicine, Jilin University, Changchun, Jilin 130021; [3]Department of Intervention, Jilin Municipal People's Hospital, Jilin, Jilin 132000, P.R. China

Received August 16, 2017; Accepted December 12, 2017

DOI: 10.3892/or.2017.6164

Abstract. Recent studies have revealed that a small amount of cisplatin can penetrate into the nucleus and induce intranuclear DNA damage. Specifically, most cisplatin accumulates in and stresses different organelles, including mitochondria, endoplasmic reticulum (ER) and the cytosol, where apoptosis signaling is activated and magnified. Bcl-2, which is mainly localized to ER and mitochondria, is identified as a key regulator of survival and apoptosis. Bcl-2 is reported to block cisplatin-induced apoptosis via regulating Ca^{2+} signaling in a variety of cancer cell lines. However, its target molecule and the mechanism responsible for its inhibitory effect in ovarian cancer are undefined. The present study revealed that Bcl-2 overexpression reduced cisplatin-induced growth inhibition and apoptosis in SKOV3 human ovarian cancer cells. Furthermore, Bcl-2 inhibited cisplatin-induced Ca^{2+} release from the ER to the cytoplasm and mitochondria, which reduced cisplatin-induced ER stress-mediated apoptosis through the mitochondrial apoptotic pathway. The overexpression of Bcl-2 inhibited the cisplatin-induced increase in the number of ER-mitochondrial contact sites in SKOV3 human ovarian cancer cells. In addition, the present study provided evidence that Bcl-2 reduced the anticancer activity of cisplatin towards ovarian cancer cells *in vivo*. These results revealed that Bcl-2 attenuates cisplatin cytotoxicity via downregulating ER-mitochondrial Ca^{2+} signaling transduction. Thus, Bcl-2 which may be a potential therapeutic target for ovarian cancer.

Correspondence to: Dr Ye Xu, Key Laboratory of Colleges and Universities of Jilin, College of Basic Medicine, Jilin Medical University, 5 Jilin Street, Jilin, Jilin 132013, P.R. China
E-mail: xuye_9707@163.com

*Contributed equally

Key words: Bcl-2, cisplatin cytotoxicity, ER-mitochondrial contact sites, Ca^{2+} signaling transduction, ovarian cancer

Introduction

Ovarian cancer is a common gynecological cancer that causes a large number of deaths in women worldwide (1,2). Epithelial ovarian cancer is the most common type, accounting for over 75% of ovarian malignancies. The symptoms for patients with early (International Federation of Gynecology and Obstetrics; FIGO I-II) and advanced (FIGO III-IV) stages of disease are significantly different (2). Despite this, 80% of epithelial ovarian cancer cases are diagnosed at an advanced stage. Chemotherapy is currently the standard treatment for epithelial ovarian cancer patients. Cisplatin is among the most widely used chemotherapeutic agents and has demonstrated significant efficacy against ovarian cancer. However, the majority of ovarian cancer patients acquire resistance to cisplatin during therapy, which represents a major obstacle to the clinical application of cisplatin (3). Therefore, the cellular and molecular mechanisms of cisplatin in ovarian cancer need to be elucidated. Bcl-2, the founding member of the Bcl-2 protein family, has anti-apoptotic activity and is overexpressed in many types of cancers. There is a growing body of evidence indicating that Bcl-2 overexpression is implicated in cisplatin resistance in ovarian cancer. However, the mechanisms responsible for this activity are undefined (4).

Numerous studies have demonstrated that Bcl-2 functions in the mitochondria and it also has an established anti-apoptotic role in the endoplasmic reticulum (ER). The anti-apoptotic function of Bcl-2 is mediated by its effects on intracellular Ca^{2+} homeostasis and dynamics (5). Ca^{2+} is an important second messenger involved in regulating cell survival and apoptosis. ER, the major intracellular Ca^{2+} storage organelle, is involved in several biological processes. Various stimuli directly target the ER to induce Ca^{2+} release into the cytosol and mitochondria, thus inducing cytosolic and mitochondrial Ca^{2+} overload and contributing to the induction of apoptosis (6). Ca^{2+} release from the ER is mainly mediated by the inositol 1,4,5-trisphosphate receptor (IP3R), an IP3-gated Ca^{2+} channel located on the surface of the ER. Bcl-2 physically interacts with IP3R to prevent pro-apoptotic Ca^{2+} transfer to the cytoplasm and mitochondria (7). Mitochondrial Ca^{2+} overload is detrimental to its function by inducing mitochondrial permeability transition pore (mPTP) opening and

loss of the mitochondrial membrane potential ($\Delta\psi m$), which triggers mitochondrial-mediated apoptosis. Ca^{2+} entry into the mitochondria is mainly mediated by voltage-dependent anion channel 1 (VDAC1), an outer mitochondrial membrane protein (8). Bcl-2 prevents mitochondrial Ca^{2+} overload and cell death through binding to VDAC1 (9). However, it remains unclear whether Bcl-2 contributes to cisplatin resistance in ovarian cancer cells via inhibiting the ER Ca^{2+} release.

Ca^{2+} release from the ER to the mitochondria regulates several mitochondrial processes (10). Notably, there is a tight interplay between the ER and mitochondria in all eukaryotic cells. The contact site between the ER and mitochondria, known as the mitochondrial-associated membrane or MAM, is a signaling hub for Ca^{2+} transfer between these organelles (11-13). ER- and mitochondrial-associated proteins including IP3R, VDAC1 and Grp75 are the basic components of the MAM. MAM provides a platform to coordinate the release of Ca^{2+} from the ER and the uptake of efficient mitochondrial Ca^{2+} (14). Arruda *et al* (15) reported that obesity leads to increased mitochondrial Ca^{2+} levels via direct uptake through the MAM junctions and not by the release of Ca^{2+} into the cytosol followed by mitochondrial uptake. Recent studies have revealed that MAM can enhance apoptosis sensitivity by increasing the transfer of Ca^{2+} into the mitochondria (16). However, whether Bcl-2 promotes cisplatin resistance via modulating ER-mitochondrial Ca^{2+} signaling remains unclear.

The aim of the present study was to determine whether Bcl-2 reduces cisplatin cytotoxicity in SKOV3 cells by blocking ER-mitochondrial Ca^{2+} signaling. Stable Bcl-2 overexpression in SKOV3 cells reduced the anticancer effects of cisplatin both *in vitro* and *in vivo*, indicating a novel therapeutic target for gene therapy in ovarian cancer.

Materials and methods

Antibodies (Abs) and drugs. Anti-caspase-3 (sc-7272; murine Ab; 1:200 dilution), anti-caspase-4 (sc-56056; murine Ab; 1:200 dilution), anti-cleaved caspase-4 (sc-22173-R; rabbit Ab; 1:200 dilution) and anti-caspase-9 (sc-56073; murine Ab; 1:200 dilution) Abs were purchased from Santa Cruz Biotechnology (Santa Cruz, CA, USA). Anti-cleaved caspase-3 (ab2302; rabbit Ab; 1:200 dilution), anti-cleaved caspase-9 (ab2324; rabbit Ab; 1:400 dilution), anti-PDI (ab2792; murine Ab; 1:1,000 dilution), anti-VDAC1 (ab14734; murine Ab; 1:1,000 dilution), anti-CHOP (ab11419; murine Ab; 1:1,000 dilution), anti-IP3R (ab5804; rabbit Ab; 1:1,000 dilution) and 2-aminoethyl diphenylborinate (2-APB, ab120124) Abs were purchased from Abcam Ltd. (Hong Kong, China). Anti-β-actin (60008-1-Ig; murine Ab; 1:2,000 dilution), anti-Bax (50599-2-Ig; rabbit Ab; 1:2,000 dilution), anti-Bcl-2 (12789-1-AP; rabbit Ab; 1:1,000 dilution), anti-cytochrome *c* (cyto *c*) (10993-1-AP; rabbit Ab; 1:1,000 dilution), anti-Grp78/BIP (11587-1-AP; rabbit Ab; 1:1,000 dilution), peroxidase-conjugated AffiniPure goat anti-mouse IgG (H+L) (SA00001-1; goat Ab; 1:2,000 dilution) and peroxidase-conjugated AffiniPure goat anti-rabbit IgG (H+L) (SA00001-2; goat Ab; 1:2,000 dilution) Abs were purchased from ProteinTech Group, Inc. (Chicago, IL, USA). The anti-calpain-1 catalytic subunit (#31038-1; rabbit Ab; 1:4,000 dilution) Ab was purchased from Signalway Antibody LLC (SAB; College Park, MD, USA). Cisplatin was purchased from Sigma-Aldrich (St. Louis, MO, USA) and dissolved in normal saline (NS) for *in vitro* use and animal studies.

Cell culture. SKOV3 ovarian cancer cells were obtained from the Chinese Academy of Medical Sciences (Beijing, China). Transfected SKOV3 cells were maintained in Roswell Park Memorial Institute (RPMI)-1640 culture (RPMI-1640; Gibco; Thermo Fisher Scientific, Inc., Carlsbad, CA, USA) and supplemented with 10% (v/v) fetal calf serum (FCS; Gibco; Thermo Fisher Scientific, Inc.) 100 mg/ml streptomycin and 100 U/ml penicillin (each from Genview, Galveston, TX, USA). The cells were incubated at 37˚C in an atmosphere containing 5% CO_2.

Transfection. SKOV3 cells were seeded at $2x10^5$ cells/well in a 24-well plate and grown until they reached 30-40% confluency before transfection. The pcDNA3.1(+) or pcDNA3.1(+)-Bcl-2 plasmids were directly transfected into the cells using Lipofectamine™ 2000 Transfection Reagent (Invitrogen Life Technologies, Carlsbad, CA, USA) according to the manufacturer's protocol. Selection was performed 72 h later using media that contained G418 (400 μg/ml). The culture continued for 14 days to generate stable transfectants and G418-resistant clones were isolated. The clones were further expanded and analyzed using western blotting. The transfected cells were used for subsequent experiments.

Cell viability assay. Cell viability was determined by 3-(4,5-dimethylthiazol-2-yl)-2,5-diphenyltetrazolium bromide (MTT) assays. The cells were plated at $1x10^4$ cells/well in 96-well plates. The following day, cisplatin was added to the wells and incubated for 24 h. Each treatment was repeated in three independent tests. MTT (20 μl) was added to each well (MTT; Sigma-Aldrich) and incubated for 4 h. Subsequently 150 μl dimethyl sulphoxide (DMSO) was added to dissolve the formazan crystals. Absorbance was assessed with a Vmax Microplate Reader (Molecular Devices, LLC, Sunnyvale, CA, USA) at a wavelength of 570 nm.

Annexin V and cell death assay. The Muse™ Annexin V Dead Cell Assay kit (Ref. MCH 100105; Merck Millipore, Darmstadt, Germany) was used to monitor cell death. Exponentially growing SKOV3/DDP cells were seeded into 6-well culture plates at a density of $2x10^5$ cells/well. After exposure to different experimental conditions for 24 h, the cells were trypsinized and resuspended in RPMI-1640 with 10% FBS at a concentration of $1x10^6$ cells/ml. The cells were incubated with Annexin V and Dead Cell Reagent in the dark at room temperature for 20 min. Finally, the samples were assessed by flow cytometry (Muse Cell Analyzer; Merck Millipore).

Calcium concentration analysis. The cytoplasmic Ca^{2+}-sensitive fluorescent dye Fluo-4/AM (Molecular Probes) and the mitochondrial Ca^{2+}-sensitive fluorescent dye Rhod-2/AM (AAT Bioquest, Inc., Sunnyvale, CA, USA) were used to determine the Ca^{2+} concentration according to the manufacturer's instructions. Before exposure to different experimental conditions for 24 h, the cells were incubated with Fluo-4/AM

or Rhod-2/AM for 30 min at 37˚C. The cell samples were then analyzed by confocal laser microscopy. All experiments were performed in triplicate.

Mitochondrial membrane potential (Δψm). Changes in the Δψm during the early stages of apoptosis were assayed using the Muse MitoPotential Assay kit (Ref. MCH 100110; Merck Millipore) in cells treated with cisplatin for 6 h. Briefly, the cells were harvested and the cell pellet was suspended in assay buffer ($1x10^5$ cells/100 μl). The MitoPotential dye working solution was added and the cell suspension was incubated at 37˚C for 20 min. After the addition of Muse MitoPotential 7-AAD dye (propidium iodide) and incubation for 5 min, changes in the Δψm and in cellular plasma-membrane permeabilization were assessed on the basis of the fluorescence intensities of both dyes, which were analyzed by flow cytometry (Muse Cell Analyzer; Merck Millipore).

Immunofluorescence staining and confocal laser microscopy. The colocalization of IP3R and VDAC1 and the expression of calpain-1 were examined by the indirect immunofluorescence method. The cells were cultured on coverslips overnight, then treated with the indicated drugs for 24 h and rinsed with 0.1 M PBS three times. After incubation, the cells were fixed with 4% paraformaldehyde for 20 min, permeabilized with 0.1% Triton X-100 (Sigma-Aldrich) for 5 min, washed three times with 0.01 M phosphate-buffered saline (PBS) and then blocked for 30 min in 5% (w/v) non-immune animal serum (goat; Beyotime Institute of Biotechnology, Shanghai, China) PBS and incubated with primary antibodies (IP3R, VDAC1 and PDI) overnight at 4˚C. The following day, the slides were incubated with the Alexa Fluor-488/546-conjugated secondary antibody (1:400 dilution; Invitrogen Life Technologies) for 1 h, and then stained with Hoechst 33342 (2 μg/ml) for 2 min and washed three times with PBS. After mounting, the cells were examined by Olympus FV1000 (Olympus, Tokyo, Japan) confocal laser microscopy.

Protein preparation and western blot analysis. The cells were treated with the indicated drugs for 24 h and various cells were harvested and lysed in lysis buffer (50 mM Tris-HCl, 1% NP40, 150 mM NaCl, 1 mM EDTA and 1 mM PMSF) for 30 min at 4˚C. Total cell extracts were separated using 12% SDS/PAGE gels and transferred to polyvinylidene fluoride (PVDF) membranes. The membranes were blocked with 3% BSA and incubated with primary antibodies diluted in blocking solution. The signals were visualized using the chemiluminescent substrate method and the SuperSignal West Pico kit (Pierce; Thermo Fisher Scientific). β-actin was used as an internal control to normalize the loading materials.

Transmission electron microscopy. The cells were treated with the indicated drugs for 24 h and were fixed with 2% paraformaldehyde and 2% glutaraldehyde in 0.1 M phosphate buffer (pH 7.4) and then post fixed with 1% OsO_4 for 2 h. The cells were dehydrated with increasing concentrations of alcohol (30, 50, 70, 90 and 100%), infiltrated with LR white resin (62661; Sigma-Aldrich) twice for 1 h and embedded in LR white resin. The solidified blocks were cut into 60-nm thicknesses and stained with uranyl acetate and lead citrate. Samples were observed under a transmission electron microscope (Hitachi H-7600; Hitachi High-Technologies Corp., Tokyo, Japan).

Human tumor xenografts. BALB/c nude mice (4-6 weeks old) were purchased from Beijing Vital River Laboratory Animal Technology Co., Ltd. (Beijing, China). The animals were maintained in specific pathogen-free conditions and in a controlled-light and humidity environment. The animal experiments were conducted in accordance with the National Institutes of Health Guide for the Care and Use of Laboratory Animals. The transfected SKOV3 cells ($5x10^6$) were subcutaneously injected into the right flank of each mouse. Tumor volume (mm^3) was assessed every two days using a Vernier caliper and calculated as follows: 0.4 x (short length)^2 x long length. Treatment was initiated when the tumors reached a volume of 30 mm^3 (on the 10th day). The mice received NS intraperitoneally [(i.p.), daily)] or 4 mg/kg cisplatin (i.p., every other day) for 8 days. The mice were sacrificed and the experiment was terminated at the end of the 18th day. The tumors were isolated, weighed and imaged.

Immunohistochemistry. Immunohistochemical staining for cleaved caspase-3 was performed on 5-μm thick sections embedded in paraffin after formalin fixation. The sections were de-paraffinized in xylene and rehydrated in graded ethanol solutions (reducing concentration from 95 to 70%). The sections were incubated in H_2O_2 solution (3% H_2O_2 in PBS buffer) for 30 min to block endogenous peroxidase activity. Antigen retrieval was performed in retrieval buffer (pH 9.0, 20 mM Tris, 0.05 mM EDTA, 0.05% Tween-20 buffer) in a 99˚C bath for 20 min. The sections were subsequently incubated at 4˚C overnight with anti-cleaved caspase-3. After rinsing with PBS buffer, the secondary antibody (MaxVision™ HRP-Polymer Anti-Rabbit IHC kit; Maixin Bio, Beijing, China) was applied for 15 min at room temperature (RT). The DAB (Maixin Bio) solution was used as the chromogen. Finally, the sections were counterstained with hematoxylin (Sigma-Aldrich) to identify the nuclei. The images were captured and analyzed using a microscope (Leica DM4000 B; Leica Microsystems GmbH, Wetzlar, Germany) with Image-Pro Plus 6.0 software (Media Cybernetics, Rockville, MD, USA).

Statistical analysis. Data are presented as the mean ± standard error (SE). The significance of the difference in mean values within and among multiple groups was examined with an ANOVA for repeated measures followed by a Duncan's post hoc test. Student's t-test was used to evaluate the significance of differences between two groups of experiments (SigmaStat; SPSS, Inc., Chicago, IL, USA). A P-value <0.05 was considered to indicate a statistically significant difference.

Results

Bcl-2 overexpression reduces cisplatin-induced growth inhibition and apoptosis in SKOV3 cells. To study the effect of Bcl-2 on cisplatin-induced growth inhibition and apoptosis, we constructed a SKOV3 cell line stably overexpressing Bcl-2 by pcDNA3.1(+)-Bcl-2 plasmids. Western blot analysis verified that SKOV3 cells transfected with pcDNA3.1(+)-Bcl-2

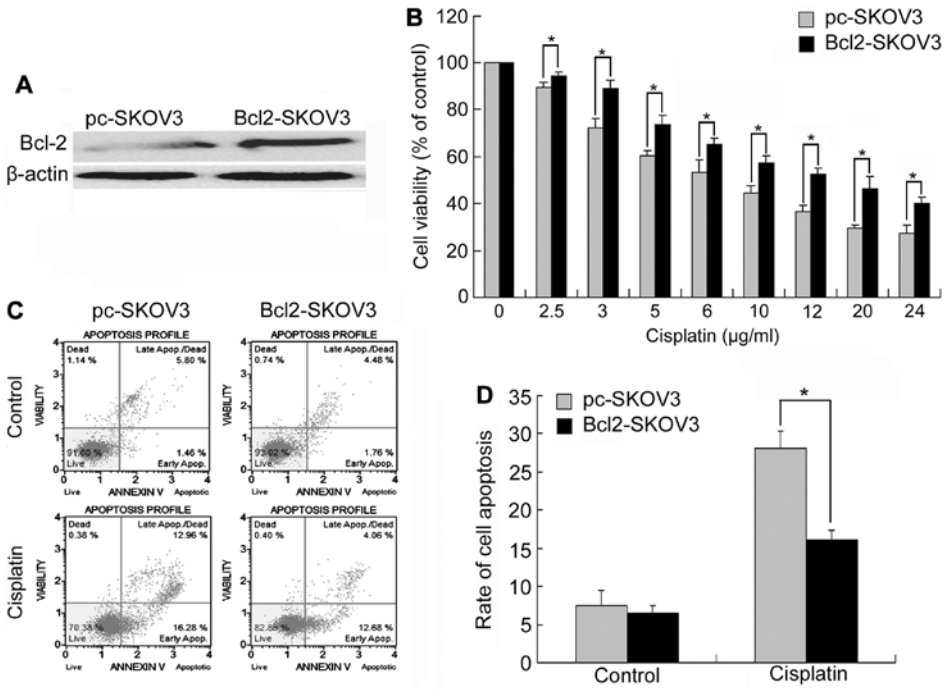

Figure 1. Bcl-2 overexpression reduces cisplatin-induced growth inhibition and apoptosis in SKOV3 cells. (A) Western blot analysis of the expression of Bcl-2 in pc-SKOV3 and Bcl-2-SKOV3 cells. (B) Pc-SKOV3 and Bcl-2-SKOV3 cells were treated with the indicated doses of cisplatin for 24 h, and then the cell viability was determined by an MTT assay. (C and D) Pc-SKOV3 and Bcl-2-SKOV3 cells were treated with 6 μg/ml cisplatin for 24 h. Subsequently, the cells were stained with Annexin V and 7-AAD and the apoptotic rate was assessed by flow cytometry. The results are the mean ± SD of three independent experiments. *P<0.05.

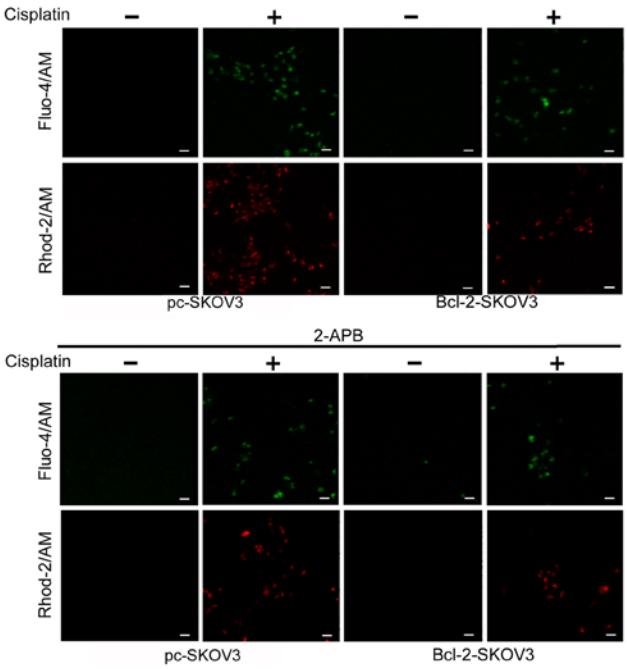

Figure 2. Bcl-2 overexpression reduces cisplatin-induced Ca^{2+} release from the ER to the cytoplasm and mitochondria. Pc-SKOV3 and Bcl-2-SKOV3 cells were treated with 6 μg/ml cisplatin for 24 h. Subsequently, the cells were loaded with Fluo-4/AM and Rhod-2/AM for 30 min and fluorescence intensity in the cytoplasm and mitochondria was assessed by confocal microscopy (scale bar, 50 μm). The results are the mean ± SD of three independent experiments. ER, endoplasmic reticulum.

(Bcl-2-SKOV3 cells) had higher levels of Bcl-2 compared with those transfected with pcDNA3.1(+) (pc-SKOV3 cells) (Fig. 1A). We treated Bcl-2-SKOV3 and pc-SKOV3 cells with 0-24 μg/ml cisplatin for 24 h and then assessed cell viability using MTT assays. Although cisplatin inhibited the growth and viability of both cell lines in a dose-dependent manner, Bcl2-SKOV3 cells were more resistant to cisplatin than pc-SKOV3 cells (Fig. 1B).

Subsequently, we treated both cell lines with 6 μg/ml cisplatin for 24 h, and then assessed the levels of apoptosis by flow cytometry. Cisplatin induced a higher apoptosis rate in the pc-SKOV3 cells than in the Bcl2-SKOV3 cells (Fig. 1C and D). In conclusion, Bcl-2 inhibited cisplatin-induced apoptosis in SKOV3 cells.

Bcl-2 overexpression reduces cisplatin-induced Ca^{2+} release from the ER to the cytoplasm and mitochondria. Previous studies indicate that Bcl-2 modulates cytosolic and mitochondrial Ca^{2+} levels in cancer cells (17). We assessed the relative cytosolic and mitochondrial Ca^{2+} levels in Bcl-2-SKOV3 and pc-SKOV3 cells treated with 6 μg/ml cisplatin for 24 h using the Fluo-4/AM and Rhod-2/AM indicators, respectively. Cisplatin treatment induced higher cytosolic and mitochondrial Ca^{2+} levels in pc-SKOV3 cells than in Bcl-2-SKOV3 cells (Fig. 2, upper panel). In order to demonstrate that cisplatin-induced cytosolic and mitochondrial Ca^{2+} accumulation derives from the ER, the IP3R chelator 2-APB was administered to both cell types in the presence and absence of cisplatin. Confocal microscopy revealed that 2-APB inhibited cisplatin-induced cytosolic and mitochondrial Ca^{2+} accumulation in both cell types (Fig. 2, lower panel). These findings demonstrated that Bcl-2 overexpression reduced cisplatin-induced Ca^{2+} release from the ER to the cytoplasm and mitochondria.

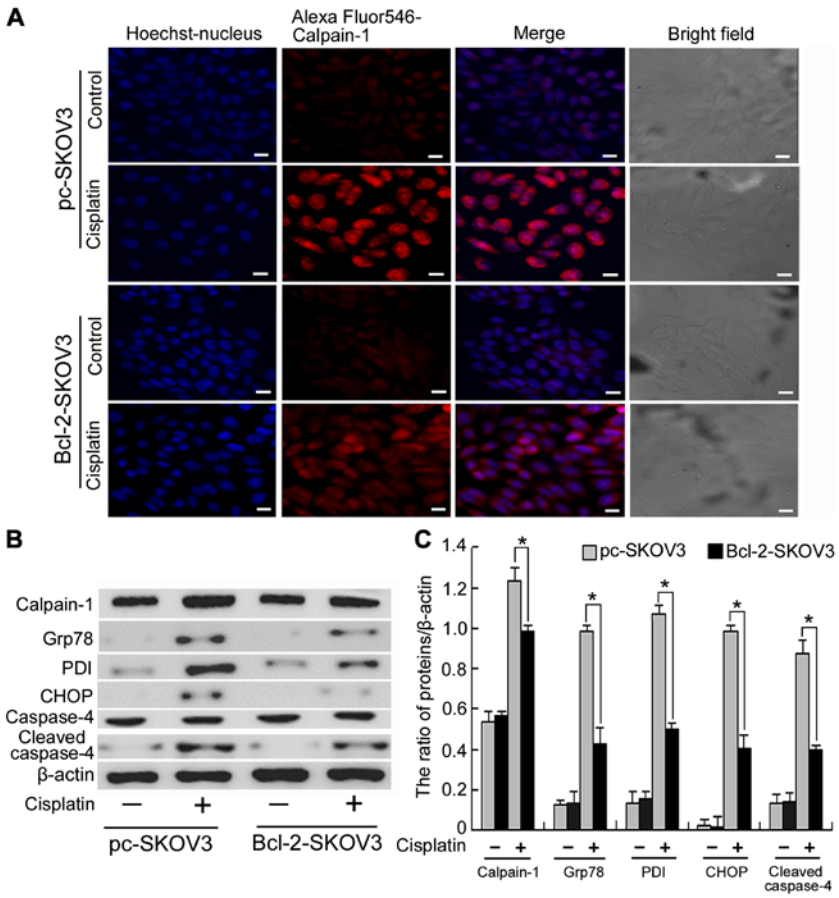

Figure 3. Bcl-2 overexpression inhibits activation of ER stress-mediated apoptosis by cisplatin in SKOV3 cells. (A) Pc-SKOV3 and Bcl-2-SKOV3 cells were treated with 6 μg/ml cisplatin for 24 h. Calpain-1 expression was observed by confocal microscopy (scale bar, 10 μm). (B and C) Western blot analysis of calpain-1, PDI, Grp78, CHOP and cleaved caspase-4 levels in pc-SKOV3 and Bcl-2-SKOV3 cells after cisplatin treatment. Results are the mean ± SD of three independent experiments. *P<0.05.

Bcl-2 overexpression inhibits the activation of ER stress-mediated apoptosis by cisplatin in SKOV3 cells. Calpain-1, a Ca^{2+}-activated protease, is involved in many cellular events and is activated by cytosolic Ca^{2+} accumulation (18). As previously demonstrated Bcl-2 inhibits cisplatin-induced cytosolic Ca^{2+} accumulation. Hence, we investigated whether Bcl-2 inhibits cisplatin-induced calpain-1 expression in SKOV3 cells. Confocal microscopy revealed that cisplatin induced higher levels of calpain-1 expression in pc-SKOV3 cells than in Bcl-2-SKOV3 cells (Fig. 3A), indicating that Bcl-2 inhibits cisplatin-induced calpain-1 expression. Calpain-1 induces ER stress by promoting the unfolded protein response. Subsequently, we assessed the expression levels of calpain-1 and the ER stress markers PDI and Grp78 in pc-SKOV3 and Bcl-2-SKOV3 cells treated with cisplatin. Western blot analysis revealed that cisplatin induced higher levels of all three proteins in pc-SKOV3 cells than in Bcl2-SKOV3 cells (Fig. 3B and C). In addition, CHOP and cleaved caspase-4 are required for the ER stress-mediated apoptosis. Cisplatin induced higher CHOP and cleaved caspase-4 levels in pc-SKOV3 cells than in Bcl-2-SKOV3 cells (Fig. 3B and C). These data indicated that Bcl-2 inhibited induction of calpain-1 expression and activation of ER stress-mediated apoptosis by cisplatin.

Bcl-2 overexpression inhibits the activation of the mitochondrial apoptosis pathway by cisplatin in SKOV3 cells. As mitochondrial Ca^{2+} overload is the major cause of decreased $\Delta\psi m$, we assessed $\Delta\psi m$ in Bcl-2-SKOV3 and pc-SKOV3 cells treated with cisplatin using flow cytometry. The results indicated that Bcl-2 inhibited the cisplatin-induced decrease in $\Delta\psi m$ in SKOV3 cells (Fig. 4A). Decreased $\Delta\psi m$ can lead to mitochondrial swelling and mitochondrial membrane rupture, which increases cytochrome *c* efflux from the mitochondria, thus, activating the mitochondrial apoptosis pathway. Subsequently, we assessed mitochondrial apoptosis by analyzing the expression of cytochrome *c*, Bcl-2, Bax, cleaved caspase-9 and cleaved caspase-3. Western blot analysis indicated that cisplatin induced a higher expression of cytochrome *c*, Bax/Bcl-2 ratio, cleaved caspase-9 and cleaved caspase-3 in pc-SKOV3 cells than in Bcl-2-SKOV3 cells (Fig. 4B and C), indicating that Bcl-2 inhibits the activation of the mitochondrial apoptosis pathway by cisplatin. Collectively, these results demonstrated that Bcl-2 inhibited the induction of the mitochondrial apoptosis pathway by cisplatin via altering mitochondrial Ca^{2+} levels in SKOV3 cells.

Bcl-2 overexpression blocks cisplatin-induced ER-mitochondrial interactions in SKOV3 cells. Close proximity of the organelles facilitates direct Ca^{2+} transfer from the ER to mitochondria (16). Therefore, we investigated whether Bcl-2 inhibited cisplatin-induced mitochondrial Ca^{2+} accumulation by decreasing ER-mitochondrial interactions in SKOV3 cells.

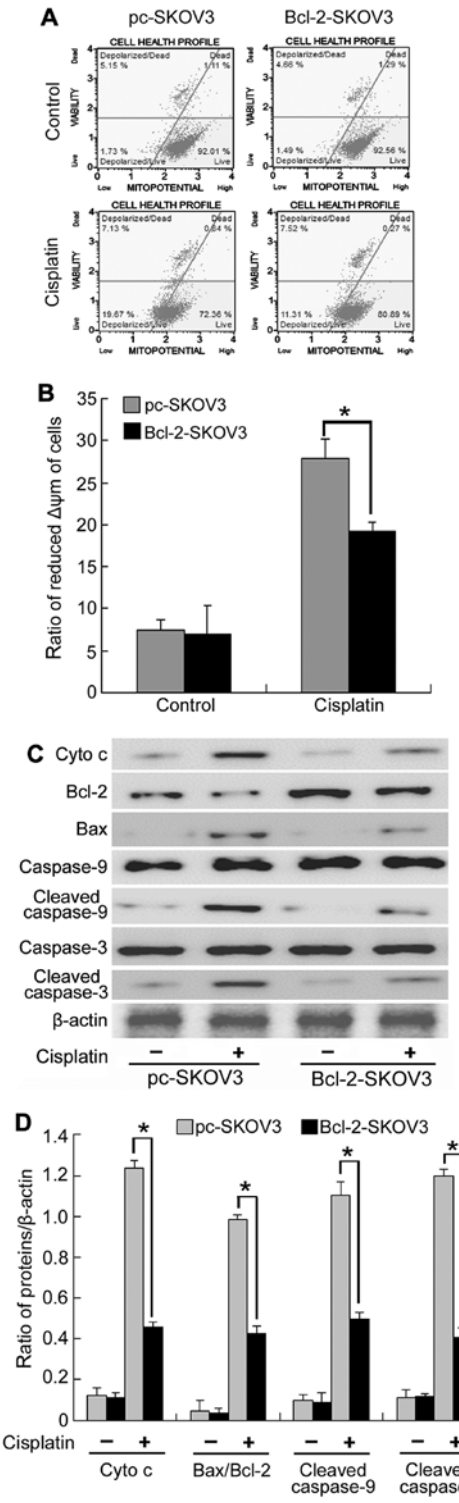

Figure 4. Bcl-2 overexpression inhibits the activation of the mitochondrial apoptosis pathway by cisplatin in SKOV3 cells. (A and B) Pc-SKOV3 and Bcl-2-SKOV3 cells were treated with 6 μg/ml cisplatin for 6 h and then stained with MitoPotential dye and 7-AAD to assess the $\Delta\psi$m by flow cytometry. (C and D) Western blot analysis of cytochrome *c*, Bcl-2, Bax, cleaved caspase-9 and cleaved caspase-3 levels in pc-SKOV3 and Bcl-2-SKOV3 cells after cisplatin treatment. The results are the mean ± SD of three independent experiments. *P<0.05.

Confocal microscopy revealed that cisplatin induced IP3R-VDAC1 colocalization to a greater extent in pc-SKOV3 cells than in Bcl-2-SKOV3 cells (Fig. 5A). Subsequently, we used electron microscopy to examine ER-mitochondrial interactions

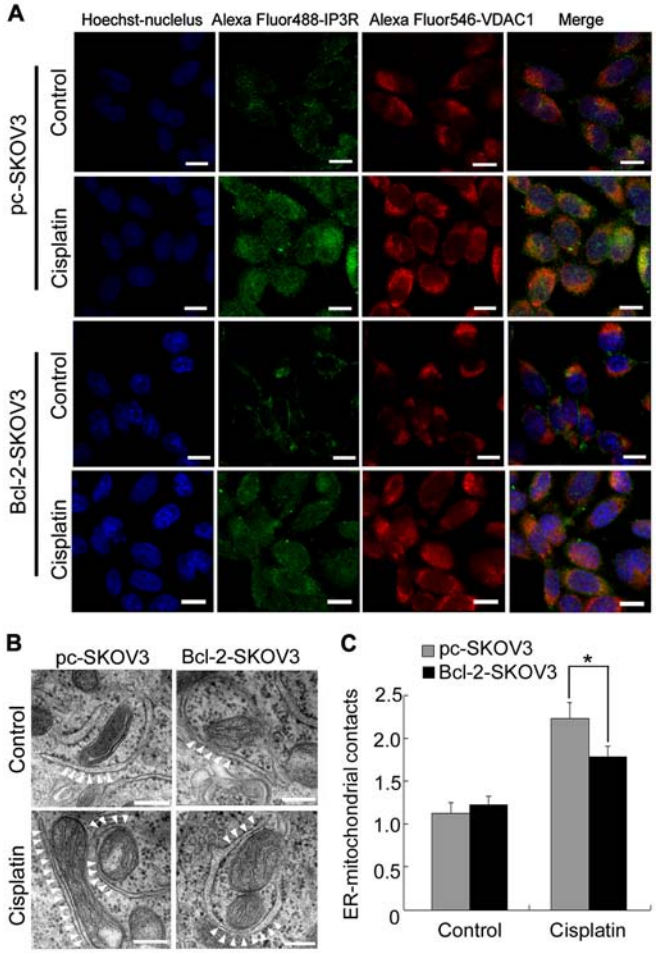

Figure 5. Bcl-2 overexpression inhibits the induction of ER-mitochondrial interactions by cisplatin in SKOV3 cells. (A) Colocalization of IP3R and VDAC1 in pc-SKOV3 and Bcl-2-SKOV3 cells after cisplatin treatment (bar, 10 μm). (B and C) Representative transmission electron microscopic photomicrographs of pc-SKOV3 and Bcl-2-SKOV3 cells treated with cisplatin for 24 h (scale bar, 200 nm). White arrowheads indicate ER-mitochondrial contacts. Results are the mean ± SD of three independent experiments. *P<0.05. ER, endoplasmic reticulum.

in pc-SKOV3 and Bcl-2-SKOV3 cells after cisplatin treatment. Significantly more contact points between the two organelles were detected in pc-SKOV3 cells than in Bcl-2-SKOV3 cells at 24 h after cisplatin treatment (Fig. 5B and C). These results revealed that Bcl-2 reduced the number of cisplatin-induced ER-mitochondrial interactions in SKOV3 cells.

Bcl-2 attenuates the in vivo antitumor activity of cisplatin in SKOV3 human ovarian cancer xenografts. To further validate the effect of Bcl-2 overexpression on cisplatin-induced SKOV3 cell apoptosis *in vivo*, we established pc-SKOV3 and Bcl-2-SKOV3 xenograft models. Mice bearing xenograft tumors were treated with NS or cisplatin for 8 days, as described in the Materials and Methods section. Cisplatin inhibited the *in vivo* growth of pc-SKOV3 xenograft tumors more efficiently than that of Bcl-2-SKOV3 cells (Fig. 6A and B). In addition, cisplatin treatment led to a greater reduction in the weight of pc-SKOV3 xenograft tumors compared with Bcl-2-SKOV3 xenograft tumors (Fig. 6C). Regarding the effects of BCL-2 overexpression on cisplatin-induced apoptosis, a greater number of cleaved caspase-3-positive cells was observed

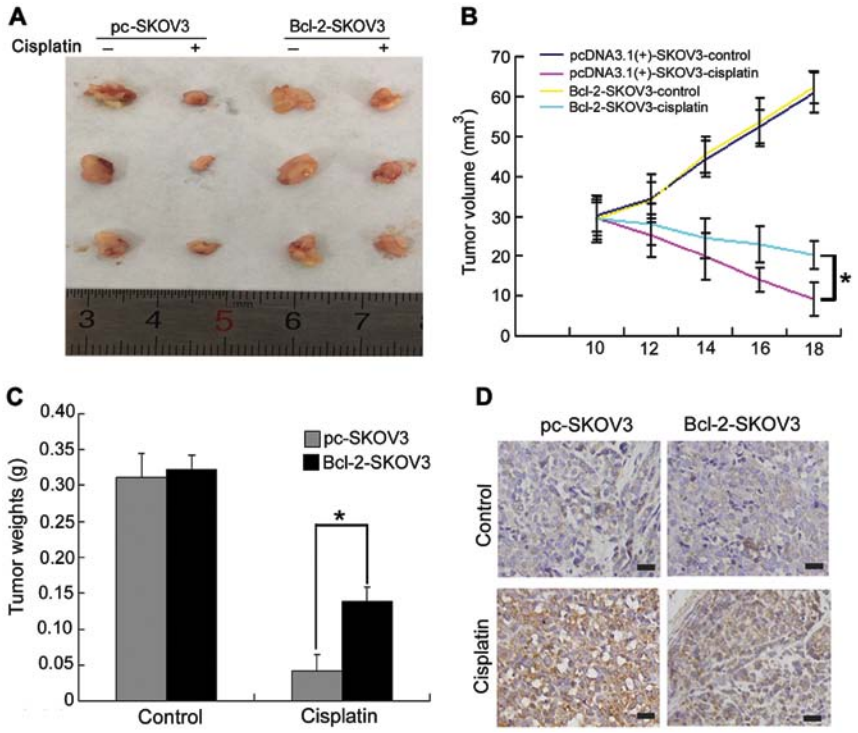

Figure 6. Bcl-2 attenuates the *in vivo* antitumor activity of cisplatin in SKOV3 human ovarian cancer xenografts. (A and B) Tumors from different treatment groups were photographed and tumor volumes were assessed on the indicated days. (C) Tumor weights were recorded. (D) The level of cleaved caspase-3 expression was evaluated immunohistochemically (scale bar, 50 μm). The results are the mean ± SD of three independent experiments. *P<0.05.

in pc-SKOV3 than in Bcl-2-SKOV3 xenograft tumors after cisplatin treatment (Fig. 6D). These data indicated that Bcl-2 attenuated the *in vivo* antitumor activity of cisplatin in ovarian xenograft tumors.

Discussion

Ovarian carcinoma is a common gynecological malignancy with an increasing incidence worldwide (2,18). Although cisplatin is one of the most widely used chemotherapeutic drugs used to treat ovarian cancer, the development of chemoresistance in ovarian cancer patients is a major problem (19). The resistance of ovarian cancer cells to cisplatin is partially dependent on Bcl-2, a prosurvival factor (20). Nishioka *et al* (21) reported that nicotine increases the resistance of H5800 lung cancer cells to cisplatin by Bcl-2 stabilization via preventing its degradation. Consistent with this findings, we demonstrated that Bcl-2 inhibited cisplatin-induced apoptosis in SKOV3 cells both *in vitro* and *in vivo* (Figs. 1 and 6). Bcl-2 overexpression suppressed the proapoptotic response to ER Ca^{2+} release and inhibited cancer cell sensitivity to various stimuli (22). In addition, the present study revealed that Bcl-2 attenuated the cisplatin-induced release of ER Ca^{2+} into the cytosol and mitochondria (Fig. 2).

Intracellular Ca^{2+} is an important second messenger with a pivotal role in signal transduction pathways that regulate a wide variety of cellular processes, including gene expression, protein synthesis and apoptosis. Cellular Ca^{2+} homeostasis is crucially important for the proper function of normal and cancer cells. Elevated intracellular Ca^{2+} levels are responsible for inducing or modulating the apoptotic response (23). Cytosolic Ca^{2+} elevation activates calpain-1, a Ca^{2+}-dependent protease. Calpain-1 overexpression is reported to promote caspase-4 activation and increase the level of ER stress-mediated apoptosis (24). Wang *et al* (25) reported that the MDL28170 (a calpain inhibitor) attenuated ER stress-mediated apoptosis by inhibiting CHOP and caspase-12. Similarly, in the present study, we found that Bcl-2 attenuated the induction of calpain-1 expression and activation of ER stress-mediated apoptosis by cisplatin (Fig. 3).

Mitochondrial Ca^{2+} uptake is essential for regulating aerobic metabolism, ATP production and cell survival. However, mitochondrial Ca^{2+} overload can lead to mitochondrial swelling and a decrease in $\Delta\psi m$, which in turn, induces the release of mitochondrial apoptotic factors (such as cytochrome *c*) into the cytosol thus activating the mitochondrial apoptosis pathway (26,27). Hu *et al* (28) reported that apigenin and 5-fu co-treatment increased mitochondrial membrane depolarization, thus inducing mitochondrial apoptosis via decreasing the Bcl-2 expression. Our data revealed that Bcl-2 attenuated cisplatin-induced decrease in $\Delta\psi m$ and cisplatin-induced elevated Bax/Bcl-2 ratio, cytochrome *c*, cleaved caspase-9 and cleaved caspase-3 expression in SKOV3 cells (Fig. 4). These results indicated that Bcl-2 attenuated cisplatin-induced activation of the mitochondrial apoptosis pathway by inhibiting ER Ca^{2+} release into the mitochondria.

Subsequently, we investigated the mechanism responsible for the Bcl-2 inhibition of cisplatin-induced ER Ca^{2+} release into the mitochondria. Recent studies revealed that MAM is crucial for the correct communication, including the efficient transmission of physiological and pathological Ca^{2+} signals, between the ER and mitochondria (29). Mitochondrial Ca^{2+} uptake mainly takes place through the MAM. Under normal physiological conditions, there is little contact between the ER and mitochondria and low physiological Ca^{2+} release maintains mitochondria function and cell survival. However, an increase in the number

of contacts between these two organelles can lead to Ca^{2+} release and thus mitochondrial Ca^{2+} overload-induced apoptosis (30-32). Notably, FATE1, a component of MAM, is reported to antagonize mitochondrial Ca^{2+} overload and chemotherapy-induced apoptosis by decreasing the number of ER-mitochondrial contacts, suggesting that MAM is responsible for mitochondrial Ca^{2+} overload-induced apoptosis (33). Our results revealed that Bcl-2 inhibited cisplatin-induced ER-mitochondrial interaction in SKOV3 cells (Fig. 5), indicating that Bcl-2 inhibits cisplatin-induced ER Ca^{2+} release into mitochondria by reducing the number of ER-mitochondrial interactions.

In conclusion, we demonstrated that Bcl-2 attenuated cisplatin-induced Ca^{2+} release from the ER into the cytosol and mitochondria, thus inhibiting cisplatin-induced ER stress-mediated apoptosis and activation of the mitochondrial apoptosis pathway. Furthermore, we revealed that decreased ER-mitochondrial crosstalk is responsible for Bcl-2 attenuation of cisplatin-induced mitochondrial Ca^{2+} accumulation in SKOV3 cells. Thus, Bcl-2 may be a novel marker of cisplatin resistance and thus, a potential therapeutic target for ovarian cancer chemotherapy.

Acknowledgements

The present study was supported by the National Nature and Science Foundation of China (NSFC 81372793) and the Department of Education of Jilin Province Project (no. 2016237). The authors would like to thank Director Dominic James from Liwen Bianji (Edanz Group China) for the language editing of this study.

References

1. Muralidhar GG and Barbolina MV: The miR-200 family: Versatile players in epithelial ovarian cancer. Int J Mol Sci 16: 16833-16847, 2015.
2. Sapiezynski J, Taratula O, Rodriguez-Rodriguez L and Minko T: Precision targeted therapy of ovarian cancer. J Control Release 243: 250-268, 2016.
3. Guo P, Xiong X, Zhang S and Peng D: miR-100 resensitizes resistant epithelial ovarian cancer to cisplatin. Oncol Rep 36: 3552-3558, 2016.
4. Dai Y, Jin S, Li X and Wang D: The involvement of Bcl-2 family proteins in AKT-regulated cell survival in cisplatin resistant epithelial ovarian cancer. Oncotarget 8: 1354-1368, 2017.
5. Hirata H, Lopes GS, Jurkiewicz A, Garcez-do-Carmo L and Smaili SS: Bcl-2 modulates endoplasmic reticulum and mitochondrial calcium stores in PC12 cells. Neurochem Res 37: 238-243, 2012.
6. Pan Z and Gollahon L: Paclitaxel attenuates Bcl-2 resistance to apoptosis in breast cancer cells through an endoplasmic reticulum-mediated calcium release in a dosage dependent manner. Biochem Biophys Res Commun 432: 431-437, 2013.
7. Cui C, Merritt R, Fu L and Pan Z: Targeting calcium signaling in cancer therapy. Acta Pharm Sin B 7: 3-17, 2017.
8. Stary CM, Sun X, Ouyang Y, Li L and Giffard RG: miR-29a differentially regulates cell survival in astrocytes from cornu ammonis 1 and dentate gyrus by targeting VDAC1. Mitochondrion 30: 248-254, 2016.
9. Arbel N and Shoshan-Barmatz V: Voltage-dependent anion channel 1-based peptides interact with Bcl-2 to prevent antiapoptotic activity. J Biol Chem 285: 6053-6062, 2010.
10. Kilpatrick BS, Yates E, Grimm C, Schapira AH and Patel S: Endo-lysosomal TRP mucolipin-1 channels trigger global ER Ca^{2+} release and Ca^{2+} influx. J Cell Sci 129: 3859-3867, 2016.
11. Theurey P, Tubbs E, Vial G, Jacquemetton J, Bendridi N, Chauvin MA, Alam MR, Le Romancer M, Vidal H and Rieusset J: Mitochondria-associated endoplasmic reticulum membranes allow adaptation of mitochondrial metabolism to glucose availability in the liver. J Mol Cell Biol 8: 129-143, 2016.
12. Area-Gomez E: Assessing the function of mitochondria-associated ER membranes. Methods Enzymol 547: 181-197, 2014.
13. Giorgi C, Wieckowski MR, Pandolfi PP and Pinton P: Mitochondria associated membranes (MAMs) as critical hubs for apoptosis. Commun Integr Biol 4: 334-335, 2011.
14. Qi H and Shuai J: Alzheimer's disease via enhanced calcium signaling caused by the decrease of endoplasmic reticulum-mitochondrial distance. Med Hypotheses 89: 28-31, 2016.
15. Arruda AP, Pers BM, Parlakgül G, Güney E, Inouye K and Hotamisligil GS: Chronic enrichment of hepatic endoplasmic reticulum-mitochondria contact leads to mitochondrial dysfunction in obesity. Nat Med 20: 1427-1435, 2014.
16. Krols M, Bultynck G and Janssens S: ER-Mitochondria contact sites: A new regulator of cellular calcium flux comes into play. J Cell Biol 214: 367-370, 2016.
17. Xie Q, Su J, Jiao B, Shen L, Ma L, Qu X, Yu C, Jiang X, Xu Y and Sun L: ABT737 reverses cisplatin resistance by regulating ER-mitochondria Ca^{2+} signal transduction in human ovarian cancer cells. Int J Oncol 49: 2507-2519, 2016.
18. Albu DF, Albu CC, Văduva CC, Niculescu M and Edu A: Diagnosis problems in a case of ovarian tumor - case presentation. Rom J Morphol Embryol 57: 1437-1442, 2016.
19. Zhu X, Ji M, Han Y, Guo Y, Zhu W, Gao F, Yang X and Zhang C: PGRMC1-dependent autophagy by hyperoside induces apoptosis and sensitizes ovarian cancer cells to cisplatin treatment. Int J Oncol 50: 835-846, 2017.
20. Tung MC, Lin PL, Cheng YW, Wu DW, Yeh SD, Chen CY and Lee H: Reduction of microRNA-184 by E6 oncoprotein confers cisplatin resistance in lung cancer via increasing Bcl-2. Oncotarget 7: 32362-32374, 2016.
21. Nishioka T, Luo LY, Shen L, He H, Mariyannis A, Dai W and Chen C: Nicotine increases the resistance of lung cancer cells to cisplatin through enhancing Bcl-2 stability. Br J Cancer 110: 1785-1792, 2014.
22. Williams A, Hayashi T, Wolozny D, Yin B, Su TC, Betenbaugh MJ and Su TP: The non-apoptotic action of Bcl-xL: Regulating Ca^{2+} signaling and bioenergetics at the ER-mitochondrion interface. J Bioenerg Biomembr 48: 211-225, 2016.
23. Shen L, Wen N, Xia M, Zhang YU, Liu W, Xu YE and Sun L: Calcium efflux from the endoplasmic reticulum regulates cisplatin-induced apoptosis in human cervical cancer HeLa cells. Oncol Lett 11: 2411-2419, 2016.
24. Ma SH, Zhuang QX, Shen WX, Peng YP and Qiu YH: Interleukin-6 reduces NMDAR-mediated cytosolic Ca^{2+} overload and neuronal death via JAK/CaN signaling. Cell Calcium 58: 286-295, 2015.
25. Wang C, Shi D, Song X, Chen Y, Wang L and Zhang X: Calpain inhibitor attenuates ER stress-induced apoptosis in injured spinal cord after bone mesenchymal stem cells transplantation. Neurochem Int 97: 15-25, 2016.
26. Demaurex N and Rosselin M: Redox control of mitochondrial calcium uptake. Mol Cell 65: 961-962, 2017.
27. Pendin D, Greotti E and Pozzan T: The elusive importance of being a mitochondrial Ca^{2+} uniporter. Cell Calcium 55: 139-145, 2014.
28. Hu XY, Liang JY, Guo XJ, Liu L and Guo YB: 5-Fluorouracil combined with apigenin enhances anticancer activity through mitochondrial membrane potential ($\Delta\Psi m$)-mediated apoptosis in hepatocellular carcinoma. Clin Exp Pharmacol Physiol 42: 146-153, 2015.
29. Galmes R, Houcine A, van Vliet AR, Agostinis P, Jackson CL and Giordano F: ORP5/ORP8 localize to endoplasmic reticulum-mitochondria contacts and are involved in mitochondrial function. EMBO Rep 17: 800-810, 2016.
30. Joshi AU, Kornfeld OS and Mochly-Rosen D: The entangled ER-mitochondrial axis as a potential therapeutic strategy in neurodegeneration: A tangled duo unchained. Cell Calcium 60: 218-234, 2016.
31. Grimm S: The ER-mitochondria interface: The social network of cell death. Biochim Biophys Acta 1823: 327-334, 2012.
32. Raturi A and Simmen T: Where the endoplasmic reticulum and the mitochondrion tie the knot: The mitochondria-associated membrane (MAM). Biochim Biophys Acta 1833: 213-224, 2013.
33. Doghman-Bouguerra M, Granatiero V, Sbiera S, Sbiera I, Lacas-Gervais S, Brau F, Fassnacht M, Rizzuto R and Lalli E: FATE1 antagonizes calcium- and drug-induced apoptosis by uncoupling ER and mitochondria. EMBO Rep 17: 1264-1280, 2016.